

1 **An intercomparison of oceanic methane and nitrous oxide measurements**

2  
3 Samuel T. Wilson<sup>1\*</sup>, Hermann W. Bange<sup>2</sup>, Damian L. Arévalo-Martínez<sup>2</sup>, Jonathan Barnes<sup>3</sup>,  
4 Alberto V. Borges<sup>4</sup>, Ian Brown<sup>5</sup>, John L. Bullister<sup>6</sup>, Macarena Burgos<sup>1,7</sup>, David W. Capelle<sup>8</sup>,  
5 Michael Casso<sup>9</sup>, Mercedes de la Paz<sup>10†</sup>, Laura Farías<sup>11</sup>, Lindsay Fenwick<sup>8</sup>, Sara Ferrón<sup>1</sup>, Gerardo  
6 Garcia<sup>11</sup>, Michael Glockzin<sup>12</sup>, David M. Karl<sup>1</sup>, Annette Kock<sup>2</sup>, Sarah Laperriere<sup>13</sup>, Cliff S.  
7 Law<sup>14,15</sup>, Cara C. Manning<sup>8</sup>, Andrew Marriner<sup>14</sup>, Jukka-Pekka Myllykangas<sup>16</sup>, John W.  
8 Pohlman<sup>9</sup>, Andrew P. Rees<sup>5</sup>, Alyson E. Santoro<sup>13</sup>, Philippe D. Tortell<sup>8</sup>, Robert C. Upstill-  
9 Goddard<sup>3</sup>, David P. Wisegarver<sup>6</sup>, Guiling L. Zhang<sup>17</sup>, Gregor Rehder<sup>12</sup>

10

11 <sup>1</sup>University of Hawai'i at Manoa, Daniel K. Inouye Center for Microbial Oceanography:  
12 Research and Education (C-MORE), Honolulu, Hawai'i, USA

13 <sup>2</sup>GEOMAR Helmholtz Centre for Ocean Research Kiel, Düsternbrooker Weg 20 24105 Kiel,  
14 Germany

15 <sup>3</sup>Newcastle University, School of Natural and Environmental Sciences, Newcastle upon Tyne,  
16 UK

17 <sup>4</sup>Université de Liège, Unité d'Océanographie Chimique, Liège, Belgium

18 <sup>5</sup>Plymouth Marine Laboratory, Plymouth, UK

19 <sup>6</sup>National Oceanic and Atmospheric Administration, Pacific Marine Environmental Laboratory,  
20 Seattle, Washington, USA

21 <sup>7</sup>Universidad de Cádiz, Instituto de Investigaciones Marinas, Departamento Química-Física  
22 Cádiz, Spain

23 <sup>8</sup>University of British Columbia, Vancouver, Department of Earth, Ocean and Atmospheric  
24 Sciences, British Columbia, Canada

25 <sup>9</sup>U.S. Geological Survey, Woods Hole Coastal and Marine Science Center, Woods Hole, USA

26 <sup>10</sup>Instituto de Investigaciones Marinas, Vigo, Spain

27 <sup>11</sup>University of Concepción, Department of Oceanography and Center for climate research and  
28 resilience (CR2), Concepción, Chile

29 <sup>12</sup>Leibniz Institute for Baltic Sea Research Warnemünde, Rostock, Germany

30 <sup>13</sup>University of California Santa Barbara, Department of Ecology, Evolution, and Marine  
31 Biology, Santa Barbara, USA

32 <sup>14</sup>National Institute of Water and Atmospheric Research (NIWA), Wellington, New Zealand

33 <sup>15</sup>Department of Chemistry, University of Otago, Dunedin, New Zealand

34 <sup>16</sup>University of Helsinki, Department of Environmental Sciences, Helsinki, Finland

35 <sup>17</sup>Ocean University of China, Department of Marine Chemistry, Qingdao, China

36

37 †Current address: Instituto Español de Oceanografía, Centro Oceanográfico de A Coruña, A

38 Coruña, Spain

39

40 \*corresponding author: stwilson@Hawai'i.edu

41 **Abstract.** Large scale climatic forcing is impacting oceanic biogeochemical cycles and is  
42 expected to influence the water-column distribution of trace gases including methane and nitrous  
43 oxide. Our ability as a scientific community to evaluate changes in the water-column inventories  
44 of methane and nitrous oxide depends largely on our capacity to obtain robust and accurate  
45 concentration measurements which can be validated across different laboratory groups. This  
46 study represents the first formal, international, intercomparison of oceanic methane and nitrous  
47 oxide measurements whereby participating laboratories received batches of seawater samples  
48 from the subtropical Pacific Ocean and the Baltic Sea. Additionally, compressed gas standards  
49 from the same calibration scale were distributed to the majority of participating laboratories to  
50 improve the analytical accuracy of the gas measurements. The computations used by each  
51 laboratory to derive the dissolved gas concentrations were also evaluated for inconsistencies (*e.g.*  
52 pressure and temperature corrections, solubility constants). The results from the intercomparison  
53 and intercalibration provided invaluable insights into methane and nitrous oxide measurements.  
54 It was observed that analyses of seawater samples with the lowest concentrations of methane and  
55 nitrous oxide had the lowest precisions. In comparison, while the analytical precision for  
56 samples with the highest concentrations of trace gases was better, the variability between the  
57 different laboratories was higher; 36% for methane and 27% for nitrous oxide. In addition, the  
58 comparison of different batches of seawater samples with methane and nitrous oxide  
59 concentrations that ranged over an order of magnitude revealed the ramifications of different  
60 calibration procedures for each trace gas. Finally, this study builds upon the intercomparison  
61 results to develop recommendations for improving oceanic methane and nitrous oxide  
62 measurements, with the aim of precluding future analytical discrepancies between laboratories.

## 63 1. Introduction

64 The increasing mole fractions of greenhouse gases in the Earth's atmosphere are causing long-  
65 term climate change with unknown future consequences. Two greenhouse gases, methane and  
66 nitrous oxide, together contribute approximately 23% of total radiative forcing attributed to well-  
67 mixed greenhouse gases (Myhre et al., 2013). It is imperative that the monitoring of methane  
68 and nitrous oxide in the Earth's atmosphere is accompanied by measurements at the Earth's  
69 surface to better inform the sources and sinks of these climatically important trace gases. This  
70 includes measurements of dissolved methane and nitrous oxide in the marine environment,  
71 which is an overall source of both gases to the overlying atmosphere (Nevison et al., 1995;  
72 Anderson et al., 2010; Naqvi et al., 2010; Freing et al., 2012; Ciais et al., 2014).

73 Oceanic measurements of methane and nitrous oxide are conducted as part of established  
74 time-series locations, along hydrographic survey lines, and during disparate oceanographic  
75 expeditions. Within low to mid-latitude regions of the open ocean, the surface waters are  
76 frequently slightly super-saturated with respect to atmospheric equilibrium for both methane and  
77 nitrous oxide. There is typically an order of magnitude range in concentration along a vertical  
78 water-column profile at any particular open ocean location (e.g. Wilson et al., 2017). In contrast  
79 to the open ocean, near-shore environments, which are subject to river inputs, coastal upwelling,  
80 benthic exchange and other processes, have higher concentrations and greater spatial and  
81 temporal heterogeneity (e.g. Schmale et al., 2010; Upstill-Goddard and Barnes, 2016).

82 Methods for quantifying dissolved methane and nitrous oxide have evolved and somewhat  
83 diverged since the first measurements were made in the 1960s (Craig and Gordon 1963;  
84 Atkinson and Richards 1967). Some laboratories employ purge-and-trap methods for extracting  
85 and concentrating the gases prior to their analysis (e.g. Zhang et al., 2004; Bullister and  
86 Wisegarver, 2008; Capelle et al., 2015; Wilson et al., 2017). Others equilibrate a seawater  
87 sample with an overlying headspace gas and inject a fixed volume of the gaseous phase into a  
88 gas analyzer (e.g. Upstill-Goddard et al., 1996; Walter et al., 2005; Farias et al., 2009). The  
89 purge and trap technique is typically more sensitive by 1-2 orders of magnitude over headspace  
90 equilibrium (Magen et al., 2014; Wilson et al., 2017). However, the purge and trap technique  
91 requires more time for sample analysis and it is more difficult to automate the injection of  
92 samples into the gas analyzer. Headspace equilibrium sampling is most suited for volatile  
93 compounds that can be efficiently partitioned into the headspace gas volume from the seawater

94 sample. Its limited sensitivity can be compensated by large volume analysis (*e.g.* Upstill-  
95 Goddard et al., 1996). Additional developments for continuous underway surface seawater  
96 measurements use equilibrator systems of various designs coupled to a variety of detectors (*e.g.*  
97 Weiss et al., 1992; Butler et al., 1989; Gülzow et al., 2011; Arévalo-Martínez et al., 2013).  
98 Determining the level of analytical comparability between different laboratories for discrete  
99 samples of methane and nitrous oxide is an important step towards improved comprehensive  
100 global assessments. Such intercomparison exercises are critical to determining the spatial and  
101 temporal variability of methane and nitrous oxide across the world oceans with confidence, since  
102 no single laboratory can single-handedly provide all the required measurements at sufficient  
103 resolution. Previous comparative exercises have been conducted for other trace gases *e.g.* carbon  
104 dioxide, dimethylsulphide, and sulfur hexafluoride (Dickson et al., 2007; Bullister and Tanhua,  
105 2010; Swan et al., 2014) and for trace elements (Cutter et al., 2013). These exercises confirm the  
106 value of the intercomparison concept.

107 To instigate this process for methane and nitrous oxide, a series of international  
108 intercomparison exercises were conducted between 2013 and 2017, under the auspices of  
109 Working Group #143 of the Scientific Committee on Oceanic Research (SCOR) ([www.scor-](http://www.scor-int.org)  
110 [int.org](http://www.scor-int.org)). Discrete seawater samples collected from the subtropical Pacific Ocean and the Baltic  
111 Sea were distributed to the participating laboratories (Table 1). The samples were selected to  
112 cover a representative range of concentrations across marine locations, from the oligotrophic  
113 open ocean to highly productive waters, and in some instances sub-oxic, coastal waters. An  
114 integral component of the intercomparison exercise was the production and distribution of  
115 methane and nitrous oxide gas standards to members of the SCOR Working Group. The  
116 intercomparison exercise was conceived and evaluated with the following four questions in  
117 mind:

118 Q1. What is the agreement between the SCOR gas standards and the ‘in-house’ gas standards  
119 used by each laboratory?

120 Q2. How do measured values of dissolved methane and nitrous oxide compare across  
121 laboratories?

122 Q3. Despite the use of different analytical systems, are there general recommendations to reduce  
123 uncertainty in the accuracy and precision of methane and nitrous oxide measurements?

124 Q4. What are the implications of inter-laboratory differences for determining the spatial and  
125 temporal variability of methane and nitrous oxide in the oceans?  
126

## 127 **2. Methods**

### 128 **2.1 Calibration of nitrous oxide and methane using compressed gas standards**

129 Laboratory-based measurements of oceanic methane and nitrous oxide require separation of the  
130 dissolved gas from the aqueous phase, with the analysis conducted on the gaseous phase.

131 Calibration of the analytical instrumentation used to quantify the concentration of methane and  
132 nitrous oxide is nearly always conducted using compressed gas standards, the specifics of which  
133 vary between each laboratory. Therefore, the reporting of methane and nitrous oxide datasets  
134 ought to be accompanied by a description of the standards used, including their methane and  
135 nitrous oxide mole fractions, the declared accuracies, and the composition of their balance or  
136 ‘make-up’ gas. For both gases, the highest accuracy commercially available standards have  
137 mole fractions close to current day atmospheric values. These standards can be obtained from  
138 national agencies including National Oceanic and Atmospheric Administration Global  
139 Monitoring Division (NOAA GMD), the National Institute of Metrology China, and the Central  
140 Analytical Laboratories of the European Integrated Carbon Observation System Research  
141 Infrastructure (ICOS-RI). By comparison, it is more difficult to obtain highly accurate methane  
142 and nitrous oxide gas standards with mole fractions exceeding modern-day atmospheric values.  
143 This is particularly problematic for nitrous oxide due to the nonlinearity of the widely used  
144 Electron Capture Detector (ECD) (Butler and Elkins, 1991).

145 The absence of a widely available high mole fraction, high accuracy nitrous oxide gas  
146 standard was noted as a primary concern at the outset of the intercomparison exercise.  
147 Therefore, a set of high-pressure primary gas standards was prepared for the SCOR Working  
148 Group by John Bullister and David Wisegarver at NOAA Pacific Marine and Environmental  
149 Laboratory (PMEL). One batch, referred to as Air Ratio Standard (ARS), had methane and  
150 nitrous oxide mole fractions similar to modern air and the other batch, referred to as Water Ratio  
151 Standard (WRS) had higher methane and nitrous oxide mole fractions for calibration of high  
152 concentration water samples. These SCOR primary standards were checked for stability over a  
153 12 month period and assigned mole fractions on the same calibration scale, known as ‘SCOR-  
154 2016.’ A comparison was conducted with NOAA standards prepared on the SIO98 calibration

155 scale for nitrous oxide and the NOAA04 calibration scale for methane. Based on the comparison  
156 with NOAA standards, the uncertainty of the methane and nitrous oxide mole fractions in the  
157 ARS and the uncertainty of the methane mole fraction in the WRS were all estimated at better  
158 than 1%. By contrast, the uncertainty of the nitrous oxide mole fraction in the WRS was  
159 estimated at 2-3%. The gas standards were distributed to twelve of the laboratories involved in  
160 this study (Table 1). The technical details on the production of the gas standards and their  
161 assigned absolute mole fractions is included in Bullister et al. (2016).

162

## 163 **2.2 Collection of discrete samples of nitrous oxide and methane**

164 Dissolved methane and nitrous oxide samples for the intercomparison exercise were collected  
165 from the subtropical Pacific Ocean and the Baltic Sea. Pacific samples were obtained on 28  
166 November 2013 and 24 February 2017 from the Hawai'i Ocean Time-series (HOT) long-term  
167 monitoring site, Station ALOHA, located at 22.75 N, 158.00 W. The November 2013 samples  
168 are included in Figure S1 and S2 in the Supplement, but are not discussed in the main Results or  
169 Discussion because fewer laboratories were involved in the initial intercomparison, and the  
170 results from these samples support the same conclusions obtained with the more recent sample  
171 collections. Seawater was collected using Niskin-like bottles designed by John Bullister (NOAA  
172 PMEL), which help minimize contamination of trace gases, in particular chlorofluorocarbons  
173 and sulfur hexafluoride (Bullister and Wisegarver, 2008). The bottles were attached to a rosette  
174 with a conductivity-temperature-depth (CTD) package. Seawater was collected from two depths:  
175 700 m and 25 m, where the near-maximum and minimum water-column concentrations for  
176 methane and nitrous oxide at this location can be found. **The 25 m samples were always well  
177 within the surface mixed layer, which ranged from 100 to 130 m depth during sampling.**

178 Replicate samples were collected from each bottle, with one replicate reserved for analysis at the  
179 University of Hawai'i to evaluate variability between sampling bottles. Seawater was dispensed  
180 from the Niskin-like bottles using Tygon® tubing into the bottom of borosilicate glass bottles,  
181 allowing overflow of at least two sample volumes and ensuring the absence of bubbles. Most  
182 sample bottles were 240 mL in size and were sealed with no headspace using butyl-rubber  
183 stoppers and aluminum crimp-seals. A few laboratory groups requested smaller crimp-sealed  
184 glass bottles ranging from 20-120 mL in volume and two laboratories used 1 L glass bottles  
185 which were closed with a glass stopper and sealed with Apiezon® grease. Seawater samples

186 were collected in quadruplicate for each laboratory. All samples were preserved using saturated  
187 mercuric chloride solution (100  $\mu\text{L}$  of saturated mercuric chloride solution per 100 mL of  
188 seawater sample) and stored in the dark at room temperature until shipment. **The choice of**  
189 **mercuric chloride as the preservative for dissolved methane and nitrous oxide was due to its long**  
190 **history of usage. It is recognized that other preservatives have been proposed (e.g. Magen et al.,**  
191 **2014, Bussmann et al., 2015), however pending a community-wide evaluation of their**  
192 **effectiveness over a range of microbial assemblages and environmental conditions for both**  
193 **methane and nitrous oxide, it is not evident that they are a superior alternative to mercuric**  
194 **chloride.**

195 Samples from the western Baltic Sea were collected during 15-21 October 2016, onboard the  
196 R/V *Elisabeth Mann Borgese* (Table 2). Since the Baltic Sea consists of different basins with  
197 varying concentrations of oxygen beneath permanent haloclines (Schmale et al., 2010), a larger  
198 range of water-column methane and nitrous oxide concentrations were accessible for inter-  
199 laboratory comparison compared to Station ALOHA. For all seven Baltic Sea stations, the  
200 water-column was sampled into an on-deck 1,000 L water tank that was subsequently  
201 subsampled into discrete sample bottles. At three stations (BAL1, BAL3, and BAL6), the water  
202 tank was filled from the shipboard high-throughput underway seawater system. For deeper  
203 water-column sampling at the stations BAL2, BAL4, and BAL5, the water tank was filled using  
204 a pumping CTD system (Strady et al., 2008) with a flow rate of  $6 \text{ L min}^{-1}$  and a total pumping  
205 time of approximately 3 h. For the final deep water-column station, BAL7, the pump that  
206 supplied the shipboard underway system was lowered to a depth of 21 m to facilitate a shorter  
207 pumping time of approximately 20 mins. Subsampling the water tank for all samples took  
208 approximately 1 h in total and the total sampling volume was less than 100 L. To verify the  
209 homogeneity of the seawater during the sampling process, the first and last samples collected  
210 from the water tank were analyzed by Newcastle University onboard the research vessel. In  
211 contrast to the Pacific Ocean sampling, which predominantly used 240 mL glass vials, each  
212 laboratory provided their own preferred vials and stoppers for the Baltic Sea samples. Seawater  
213 samples were collected in triplicate for each laboratory. All samples were preserved with 100  
214  $\mu\text{L}$  of saturated mercuric chloride solution per 100 ml of seawater sample, with the exception of  
215 samples collected by U.S. Geological Survey, who analyzed unpreserved samples onboard the  
216 research vessel.



217

### 218 **2.3. Sample analysis**

219 Each laboratory measured dissolved methane and nitrous oxide slightly differently. A full  
220 description of each laboratory's method can be found in Table S6 and Table S7 in the  
221 Supplement for methane and nitrous oxide, respectively.

222 The majority of laboratories measured methane and nitrous oxide by equilibrating the  
223 seawater sample with an overlying headspace and subsequently injecting a portion of the gaseous  
224 phase into the gas analyzer. This method has been conducted since the 1960s when gas  
225 chromatography was first used to quantify dissolved hydrocarbons (McAuliffe, 1963). The  
226 headspace was created using helium, nitrogen, or high-purity air to displace a portion of the  
227 seawater sample within the sample bottle. Alternatively, a subsample of the seawater was  
228 transferred to a gas-tight syringe and the headspace gas subsequently added. The volume of the  
229 vessel used to conduct the headspace equilibration ranged from 20 ml borosilicate glass vials to 1  
230 L glass vials and syringes used by Newcastle University and U.S. Geological Survey,  
231 respectively. The dissolved gases equilibrated with the overlying headspace at a controlled  
232 temperature for a set period of time that ranged from 20 min to 24 h for the different laboratories.  
233 The longer equilibration times are due to overnight equilibrations in water baths. The majority  
234 of laboratories enhanced the equilibration process by some initial period of physical agitation.  
235 After equilibration, an aliquot of the headspace was transferred into the gas analyzer (GA) by  
236 either physical injection, displacement using a brine solution, or injection using a switching  
237 valve. Some laboratories incorporated a drying agent and a carbon dioxide scrubber prior to  
238 analysis. The gas sample passed through a multi-port injection valve containing a sample loop of  
239 known volume, which transferred the gas sample directly onto the analytical column within the  
240 oven of the GA. Calibration of the instrument was achieved by passing the gas standards  
241 through the injection valve.

242 The final gas concentrations using the headspace equilibration method was calculated by:

243

$$244 \quad [1] \quad C_{gas} [\text{nmol L}^{-1}] = \left( \beta x P V_{wp} + \frac{xP}{RT} V_{hs} \right) / V_{wp}$$

245

246 where  $\beta$  is the Bunsen solubility of nitrous oxide (Weiss and Price, 1980) or methane  
247 (Wiesenburg and Guinasso, 1979) in  $\text{nmol L}^{-1} \text{atm}^{-1}$ ,  $x$  is the dry gas mole fraction (ppb)

248 measured in the headspace,  $P$  is the atmospheric pressure (atm),  $V_{wp}$  is the volume of water  
249 sample (mL),  $V_{hs}$  is the volume (mL) of the created headspace,  $R$  is the gas constant (0.08205746  
250 L atm K<sup>-1</sup>mol<sup>-1</sup>), and  $T$  is equilibration temperature in Kelvin (K). An example calculation is  
251 provided in Table S8 in the Supplement.

252 In contrast to the headspace equilibrium method, five laboratories used a purge-and-trap  
253 system for methane and/or nitrous oxide analysis (Table S6 and Table S7 in the Supplement).  
254 These systems were directly coupled to a Flame Ionization Detector (FID) or ECD, with the  
255 exception of University of British Columbia, where a quadrupole mass spectrometer with an  
256 electron impact ion source and Faraday cup detector were used (Capelle et al., 2015). The  
257 purge-and-trap systems were broadly similar, each transferring the seawater sample to a sparging  
258 chamber. Sparging times typically ranged from 5-10 min and the sparge gas was either high  
259 purity helium or high purity nitrogen. **In addition to commercially available gas scrubbers,**  
260 **purification of the sparge gas was achieved by passing it through stainless steel tubing packed**  
261 **with Poropak Q and immersed in liquid nitrogen. This is a recommended precaution to**  
262 **consistently achieve a low blank signal of methane.** The elutant gas was dried using Nafion or  
263 Drierite, and subsequently cryotrapped on a sample loop packed with Porapak Q to aid retention  
264 of methane and nitrous oxide. **Cryotrapping was achieved for methane using liquid nitrogen (-**  
265 **195°C) and either liquid nitrogen or cooled ethanol (-70°C) for nitrous oxide.** Subsequently, the  
266 valve was switched to inject mode and the sample loop was rapidly heated to transfer its contents  
267 onto the analytical column. Calibration was achieved by injecting standards via sample loops  
268 using multi-port injection valves. Injection of standards upstream of the sparge chamber allowed  
269 for calibration of the purge-and-trap gas handling system, in addition to the GA. Calculation of  
270 the gas concentrations using the purge-and-trap method was achieved by application of the ideal  
271 gas law to the standard gas measurements:

$$272 \quad [2] \quad PV = nRT$$

273 where  $P$ ,  $R$ , and  $T$  are the same as Equation 1,  $V$  represents the volume of gas injected (L),  
274 and  $n$  represents moles of gas injected. Rearranging Equation 2 yields the number of moles of  
275 methane or nitrous oxide gas for each sample loop injection of compressed gas standards. These  
276 values were used to determine a calibration curve based on the measured peak areas of the  
277 injected standards, and thereafter derive the number of moles measured for each unknown  
278 sample. To calculate concentrations of methane or nitrous oxide in a water sample, the number

279 of moles measured were divided by the volume (L) of seawater sample analyzed. An example  
280 calculation is provided in Table S8 in the Supplement.

281

## 282 **2.4 Data analysis**

283 The final concentrations of methane and nitrous oxide are reported in  $\text{nmol kg}^{-1}$ . The analytical  
284 precision for each batch of samples obtained by each of the individual laboratories was estimated  
285 from the analysis of replicate seawater samples and reported as the coefficient of variation (%).

286 The values reported by each laboratory for all the batches of seawater samples are shown in  
287 Tables S1 to S4 in the Supplement. Due to the observed inter-laboratory variability, it is likely  
288 that the median value of methane and nitrous oxide for each batch of samples does not represent  
289 the absolute *in situ* concentration. As this complicates the analytical accuracy for each  
290 laboratory, we instead calculated the percentage difference between the median concentration  
291 determined for each set of samples and the mean value reported by an individual laboratory. The  
292 presence of outliers was established using the Interquartile Range (IQR) and by comparing with  
293 one standard deviation applied to the overall median value.

294

## 295 **3. Results**

### 296 **3.1 Comparison of methane and nitrous oxide gas standards**

297 Six laboratories compared their existing ‘in-house’ standards of methane with the SCOR  
298 standards. This was done by calibrating in-house standards and deriving a mixing ratio for the  
299 SCOR standards which were treated as unknowns. Four laboratories reported methane values for  
300 either the ARS or WRS within 3% of their absolute concentration, whereas two laboratories  
301 reported an offset of 6% and 10% between their in-house standards and the SCOR standards  
302 (Table S6 in the Supplement). For those laboratories who measured the SCOR standards to  
303 within 3% or better accuracy, observed offsets in methane concentrations from the overall  
304 median cannot be due to the calibration gas.

305 Seven laboratories compared their own in-house standards of nitrous oxide with the prepared  
306 SCOR standards. Six laboratories reported values of nitrous oxide for the ARS which were  
307 within 3% of the absolute concentration, with the remaining laboratory reporting an offset of  
308 10% (Table S7 in the Supplement). The majority of these laboratories (five out of six groups)  
309 compared the SCOR ARS with NOAA GMD standards, which have a balance gas of air instead

310 of nitrogen. Some laboratories with analytical systems that incorporated fixed sample loops (*e.g.*  
311 1 or 2 ml loops housed in a 6-port or 10-port injection valve) had difficulty analyzing the WRS,  
312 as the peak areas created by the high mole fraction of the standard exceeded the signal typically  
313 measured from in-house standards or acquired by sample analysis, by an order of magnitude.  
314 The high mole fraction of the WRS was not an issue when multiple sample loops of varying  
315 sizes were incorporated into the analytical system, which was the case for purge-and-trap based  
316 designs. For the two laboratories with an in-house standard of comparable mole fraction to the  
317 WRS, an offset of 3% and a >20% offset was reported.

318

### 319 **3.2 Methane concentrations in the intercomparison samples**

320 Overall, median methane concentrations in seawater samples collected from the Pacific Ocean  
321 and the Baltic Sea ranged from 0.9 to 60.3 nmol kg<sup>-1</sup> (Table 2). Out of 101 reported values, 3  
322 outliers were identified using the IQR criterion and were not included in further analysis. The  
323 methane data values for each batch of samples analyzed by each laboratory, including the mean  
324 and standard deviation, the number of samples analyzed, and the % offset from the overall  
325 median value are reported in Table S1 and Table S2 in the Supplement. Analysis conducted by  
326 the University of Hawai'i of methane and nitrous oxide from each Niskin-like bottle used in the  
327 Pacific Ocean sampling did not reveal any bottle-to-bottle differences. Furthermore, analysis by  
328 Newcastle University showed there was no difference between the first and the last set of  
329 samples collected from the 1000 L collection used in the Baltic Sea sampling.

330 The two Pacific Ocean sampling sites had the lowest water-column concentrations of  
331 methane (Fig. 1a and 1b). The PAC1 samples collected from within the mesopelagic zone,  
332 where methane concentrations have been reported to be less than 1 nmol kg<sup>-1</sup> (Reeburgh, 2007;  
333 Wilson et al., 2017), showed a distribution of reported concentrations skewed towards the higher  
334 values. For the PAC1 samples, seven out of twelve laboratories reported values  $\leq 1$  nmol kg<sup>-1</sup>  
335 and the mean coefficient of variation for all laboratories was 11% (Table 2). In contrast to the  
336 mesopelagic samples, the methane concentrations for the near-surface seawater samples (PAC2)  
337 were close to atmospheric equilibrium (Fig. 1b). Measured concentrations of methane for PAC2  
338 samples ranged from 1.9 to 3.8 nmol kg<sup>-1</sup> and the mean coefficient of variation for all  
339 laboratories was 7%. Similar to the PAC1 samples, PAC2 also had a distribution of data skewed  
340 towards the higher concentrations.

341 Three Baltic Sea sampling sites (BAL1, BAL3, and BAL6) had median methane  
342 concentrations that ranged from 4.1 to 5.7 nmol kg<sup>-1</sup> (Fig. 1c). The BAL1 samples also showed a  
343 skewed distribution of reported values towards higher concentrations, as seen in PAC1 and  
344 PAC2 samples. However, this was not evident in BAL3 or BAL6, which had the closest  
345 agreement between the reported methane concentrations. For these three sets of Baltic Sea  
346 samples, the mean coefficient of variation for all laboratories ranged from 4% (BAL3) to 9%  
347 (BAL1). The next three Baltic Sea samples (BAL4, BAL5, and BAL7) had methane  
348 concentrations that ranged from 18.8 to 35.4 nmol kg<sup>-1</sup> (Fig. 1d). These three sets of samples  
349 had a normal distribution of data and the closest agreement between the reported concentrations  
350 for all of the Pacific Ocean and Baltic Sea samples. Furthermore, for these three sets of samples,  
351 the mean coefficient of variation for all laboratories was 4% (Table 2). The final Baltic Sea  
352 sample (BAL2) had the highest concentrations of methane, with a median reported value of 60.3  
353 nmol kg<sup>-1</sup>, and a large range of values (45.2 to 67.2 nmol kg<sup>-1</sup>; Fig. 1e). The BAL2 samples had  
354 the lowest overall mean coefficient of variation for all laboratories; 2% (Table 2).

355 Further analysis of the data was conducted to better comprehend the factors that caused the  
356 observed inter-laboratory variability in methane measurements. The deviation from median  
357 values was calculated for each sample collected from the Baltic Sea (Fig. 2). The Pacific Ocean  
358 samples (PAC1 and PAC2) were not included in this analysis due to the skewed distribution of  
359 data. There were also some instances in the Baltic Sea samples, where the median concentration  
360 might not have realistically represented the absolute *in situ* methane concentration. This was  
361 most likely to have occurred at low concentrations due to the skewed distribution of reported  
362 concentrations (*e.g.* BAL1) or at high concentrations where there was a large range in reported  
363 values (*e.g.* BAL2). The results revealed that a few laboratories (Datasets D, F, and G) were  
364 consistently within or close to 5% of the median value for all batches of seawater samples (Fig.  
365 2). Some laboratories (*e.g.* Datasets B, C, and H) had a higher deviation from the median value  
366 at higher methane concentrations. Two laboratories (Datasets J and K) had a higher deviation  
367 from the median value at lower methane concentrations. Finally, in some cases it was not  
368 possible to determine a trend (Datasets A and E), due to the variability.

369 The reasons behind the trends for each dataset became more apparent when considering the  
370 effect of the inclusion or exclusion of low standards in the calibration curve on the resulting  
371 derived concentrations (Fig. 3). The FID has a linear response to methane at nanomolar values

372 and therefore a high level of accuracy across a relatively wide range of *in situ* methane  
373 concentrations can be obtained with the correct slope and intercept. To demonstrate this,  
374 calibration curves for methane were provided by the University of Hawai'i. These revealed  
375 minimal variation in the slope value when calibration points were increased from low mole  
376 fractions (Fig. 3a) to higher mole fractions (Fig. 3b). However, the intercept value was sensitive  
377 to the range of calibration values used, and this effect was further exacerbated when only the  
378 higher calibration points were included (*i.e.* Fig. 3c). **The relevance to final methane**  
379 **concentrations is demonstrated by considering the values reported by the University of Hawai'i**  
380 **for PAC2 samples (Fig. 1b). An almost 30% increase in final methane concentration occurs**  
381 **from the use of the calibration equation in Figure 3c, compared to Figure 3a. This derives from a**  
382 **measured peak area for methane of 62 for a sample with a volume of 0.076 L and a seawater**  
383 **density of 1024 kg m<sup>-3</sup>, yielding a final methane concentration of 2.1 and 2.8 nmol kg<sup>-1</sup> using the**  
384 **equations from Figure 3a and 3c, respectively. With this understanding on the effect of FID**  
385 **calibration, we consider it likely that the increased deviation from median values at high methane**  
386 **concentrations (Datasets B, C, and H) results from differences in calibration slope between each**  
387 **laboratory. In contrast, the datasets with a higher offset at low methane concentrations (Datasets**  
388 **J and K) could be due to erroneous low standard values causing a skewed intercept. In addition,**  
389 **there may be other factors including sample contamination, discussed in Section 3.4.**

390

### 391 **3.3 Nitrous oxide concentrations in the intercomparison samples**

392 Overall, median nitrous oxide concentrations in seawater samples collected from the Pacific  
393 Ocean and the Baltic Sea ranged from 3.4 to 42.4 nmol kg<sup>-1</sup> (Table 2). Of the 113 reported  
394 values, ten outliers were identified using the IQR criterion and were not included in further  
395 analysis. The nitrous oxide data values for each batch of samples analyzed by each laboratory,  
396 including the mean and standard deviation, the number of samples analyzed, and the % offset  
397 from the overall median value are reported in Table S3 and Table S4 in the Supplement.

398 For six sets of seawater samples, BAL1, BAL2, BAL3, BAL6, BAL7, and PAC2, the  
399 concentrations of nitrous oxide were close to atmospheric equilibrium. The reported values  
400 ranged from 7.7 to 12.7 nmol kg<sup>-1</sup> in the Baltic Sea (Fig. 4a) and from 5.9 to 7.6 nmol kg<sup>-1</sup> in the  
401 Pacific Ocean (Fig. 4b). For the Pacific Ocean near-surface (**mixed layer**) sampling site (PAC2),  
402 the theoretical value of nitrous oxide concentration in equilibrium with the overlying atmosphere

403 is also shown (Fig. 4b). For these six samples with concentrations close to atmospheric  
404 equilibrium, the mean coefficient of variation for all laboratories ranged from 3% (BAL3 and  
405 PAC2) to 5% (BAL1) (Table 2).

406 For the three other sets of samples (BAL4, BAL5, and PAC1), the nitrous oxide  
407 concentrations deviated significantly from atmospheric equilibrium (Fig. 4c, 4d, and 4e). At one  
408 sampling site, BAL4 (Fig. 4c), nitrous oxide was under-saturated with respect to atmospheric  
409 equilibrium and reported concentrations ranged from 2.1–5.5 nmol kg<sup>-1</sup>. As observed in the low  
410 concentration Pacific Ocean methane samples, there was a skewed distribution of the data  
411 towards the higher nitrous oxide concentrations. The BAL4 samples also had the highest  
412 variability (*i.e.* lowest precision), with a mean coefficient of variation of 8% (Table 2). The two  
413 remaining samples (PAC1 and BAL5) had much higher concentrations of nitrous oxide, as  
414 expected for low-oxygen regions of the water-column. In contrast to the samples with near  
415 atmospheric equilibrium concentrations of nitrous oxide, there was a low overall agreement  
416 between the independent laboratories for PAC1 and BAL5 nitrous oxide concentrations (Fig. 4d,  
417 4e). At PAC1 and BAL5, nitrous oxide concentrations ranged from 34.3–45.8 nmol kg<sup>-1</sup> (Fig.  
418 4d) and 30.1–45.9 nmol kg<sup>-1</sup>, respectively (Fig. 4e). The mean coefficient of variation for all  
419 laboratories was 4% for BAL5 samples compared to 3% for PAC1 samples.

420 The deviation of individual nitrous oxide concentrations from the median value provides  
421 insight into the variability associated with their measurements (Fig. 5). The BAL1 dataset was  
422 not included in this analysis due to its skewed data distribution and the high inter-laboratory  
423 variability for BAL5 indicated that the median value may differ from the absolute nitrous oxide  
424 concentration for this sample. For the low nitrous oxide Baltic Sea and Pacific Ocean samples  
425 (Fig. 5a), the majority of data points were within 5% of the median values. Furthermore, for the  
426 majority of laboratories, the data points for separate seawater samples clustered together  
427 indicating some consistency to the extent they varied from the overall median value. Exceptions  
428 to this observation include Datasets E, C, L, and K (Fig. 5a) which demonstrated varying  
429 precision and accuracy. At high nitrous oxide concentrations (Fig. 5b), there are fewer data  
430 points within 5% of the median value compared to low nitrous oxide concentrations (Fig. 5a).  
431 Therefore, for PAC1 and BAL5 samples, 6 and 7 data points fall within 5% of the median value,  
432 respectively. Furthermore, only three laboratories (Datasets F, G, and K) had data for both  
433 Pacific Ocean and Baltic Sea samples within 5% of the median value. This could have been

434 caused by inconsistent analysis between different batches of samples or by variable sample  
435 collection and transportation.

436 The likely factors that caused these offsets in nitrous oxide concentrations among  
437 laboratories include sample analysis and calibration of the gas analyzers. Calibration of the ECD  
438 is nontrivial and at least two prior publications have discussed nitrous oxide calibration issues  
439 (Butler and Elkins, 1991; Bange et al., 2001). The laboratories participating in the nitrous oxide  
440 intercomparison employed different calibration procedures (Fig. 6). Some used a linear fit and  
441 kept their analytical peak areas within a narrow range (Fig. 6a), while others used a step-wise  
442 linear fit and therefore used different slopes for low and high nitrous oxide mole fractions (Fig.  
443 6b). Finally, some applied a polynomial curve (Fig. 6c) and sometimes two different polynomial  
444 fits, for low and high concentrations. The difficulty in calibrating the ECD was evidenced by the  
445 deviation from median values as multiple datasets show good precision but consistent offsets at  
446 the lowest (Fig. 5a) and highest (Fig. 5b) final concentrations of nitrous oxide.

447

### 448 **3.4 Sample storage and sample bottle size**

449 Because prolonged storage of samples can influence dissolved gas concentrations, including  
450 methane and nitrous oxide, the intercomparison dataset was analyzed for sample storage effects  
451 (Table S5 in the Supplement). It should, however, be noted that assessing the effect of storage  
452 time on sample integrity was not a formal goal of the intercomparison exercise and replicate  
453 samples were not analyzed at repeated intervals by independent laboratories, as would normally  
454 be required for a thorough analysis. Nonetheless our results did provide some insights into  
455 potential storage-related problems. Most notably, there were indications that an increase in  
456 storage time caused increased concentrations and increased variability for methane samples with  
457 low concentrations, *i.e.* PAC1 and PAC2 samples which had median methane concentrations of  
458 0.9 and 2.3 nmol kg<sup>-1</sup>, respectively (Fig. 7). In comparison, for samples of nitrous oxide with  
459 low concentrations there was no trend of increasing values as observed for samples with low  
460 methane concentrations.

461 Another variable which differed between laboratories for the intercomparison exercise was  
462 the size of samples bottle, which ranged from 25 ml to 1 liter for the different laboratories.  
463 There was no observed difference between the methane and nitrous oxide values obtained from  
464 the various sampling bottles and it was concluded that sampling bottles were not a controlling



465 factor for the observed differences between laboratories. We note, however, the potential for  
466 greater air bubble contamination in smaller bottles.

467

#### 468 **4. Discussion**

469 The marine methane and nitrous oxide analytical community is growing. This is reflected in the  
470 increasing number of corresponding scientific publications and the resulting development of a  
471 global database for methane and nitrous oxide (Bange et al., 2009). Like all Earth observation  
472 measurements, there is a need for intercomparison exercises of the type reported here, for data  
473 quality assurance, and for appropriate reporting practices (National Research Council, 1993). To  
474 the best of our knowledge, the work presented here is the first formal intercomparison of  
475 dissolved methane and nitrous oxide measurements. Based on our results, we discuss the lessons  
476 learned and our recommendations moving forward, by addressing the four questions that were  
477 posed in the Introduction.

478

##### 479 **4.1 What is the agreement between the SCOR gas standards and the ‘in-house’ gas 480 standards used by each laboratory?**

481 It is typical for laboratories to source some, or all, of their compressed gas standards from  
482 commercial suppliers. National agencies, such as NOAA GMD or National Institute of  
483 Metrology China, also provide standards to the scientific community. The national agencies  
484 typically offer a lower range in concentrations than commercial suppliers, but their standards  
485 tend to have a higher level of accuracy. Of the twelve laboratories participating in the  
486 intercomparison, eight reported using national agency standards, with seven of them using gases  
487 sourced from NOAA GMD. Since the methane and nitrous oxide mole fractions of these  
488 national agency standards are equivalent to modern-day atmospheric mixing ratios, they are  
489 similar to the SCOR ARS distributed to the majority of laboratories in this study. Laboratories  
490 in receipt of the SCOR standards were asked to predict their mole fractions based on those of  
491 their own in-house standards. For the majority that conducted this exercise, there was good  
492 agreement (<3% difference) between the NOAA GMD and the SCOR ARS for both methane  
493 and nitrous oxide. For three laboratories, a larger offset was observed between the NOAA GMD  
494 and the SCOR ARS. There was also a good prediction for the higher methane content SCOR  
495 WRS, facilitated by the linear response of the FID (Fig. 3). In contrast, the nitrous oxide mole

496 fraction in the SCOR WRS exceeded the typical working range for several laboratories and it  
497 was difficult for them to cross-compare with their in-house standards. This reflects an analytical  
498 set-up that involves on-column injection via a 6-port or 10-port valve with one or two sample  
499 loops, respectively. The sample loops have a fixed volume and their inaccessibility makes it  
500 difficult to replace them by a smaller loop size. Therefore either dilution of the standard is  
501 required, or smaller loops need to be incorporated into the calibration protocol. The two  
502 laboratories that compared their in-house standards with the SCOR WRS reported an offset of  
503 3% and >20%. This indicates that variability between standards can be an issue for obtaining  
504 accurate dissolved concentrations and provides support for the production of a widely available  
505 high concentration nitrous oxide standard. We strongly recommend that all commercially  
506 obtained standards are cross-checked against primary standards, such as the SCOR ARS and  
507 WRS. This should be conducted at least at the beginning and end of their use to detect any drift  
508 that may have occurred during their lifetime. With due diligence and care, the SCOR standards  
509 provide the capability for cross-checking personal standards for years to decades (Bullister et al.,  
510 2016).

511

#### 512 **4.2 How do measured values of methane and nitrous oxide compare across laboratories?**

513 **Methane:** The methane intercomparison highlighted the variability that exists between  
514 measurements conducted by independent laboratories. At low methane concentrations, a skewed  
515 distribution of methane data was observed, which was particularly evident in PAC1 (Fig. 1a).  
516 Potential causes include calibration procedures (Section 3.2) and/or sample contamination which  
517 is more prevalent at low concentrations (Section 3.4). For some laboratories, the low methane  
518 concentrations are close to their detection limit, which is determined by the relatively low  
519 sensitivity of the FID and the small number of moles of methane in an introduced headspace  
520 **equilibrated** with seawater. An approximate working detection limit for methane analysis via  
521 headspace equilibration is  $1 \text{ nmol kg}^{-1}$ , although some laboratories improve upon this by having  
522 a large aqueous: gaseous phase ratio during the equilibration process (*e.g.* Upstill-Goddard et al.,  
523 1996). Depending upon the volume of sample analyzed, purge-and-trap analysis can have a  
524 detection limit much lower than  $1 \text{ nmol kg}^{-1}$  (*e.g.* Wilson et al., 2017). Methane measurements  
525 in aquatic habitats with methane concentrations near the limit of analytical detection include  
526 mesopelagic and high latitude environments distal from coastal or benthic inputs (*e.g.* Rehder et

527 al., 1999; Kitidis et al., 2010; Fenwick et al., 2017). Of additional concern is that the skewed  
528 distribution of methane concentrations also occurs in samples collected both from the surface  
529 ocean (PAC2; Fig. 1b) and coastal environments (BAL1; Fig. 1c). Methane concentrations  
530 between 2–6 nmol kg<sup>-1</sup> are within the detection limit of all participating laboratories. To address  
531 this we recommend that laboratories restrict sample storage to the minimum time required to  
532 analyze the samples and incorporate internal controls into their sample analysis (Section 4.4).

533 There was an improvement in the overall agreement between the laboratories for samples  
534 with higher methane concentrations. However, some of the highest variability between the  
535 laboratories was observed at the highest concentrations of methane analyzed (BAL2; Fig. 1e).  
536 This high degree of variability resulted in significant uncertainty in the absolute *in situ*  
537 concentration. Methane concentrations of this magnitude and higher are found in coastal  
538 environments (Zhang et al., 2004; Jakobs et al., 2014; Borges et al., 2017) and in the water-  
539 column associated with seafloor emissions (*e.g.* Pohlman et al., 2011). These environments are  
540 considered vulnerable to climate induced changes and eutrophication, and therefore it is  
541 necessary that independent measurements are conducted to the highest possible accuracy to  
542 allow for inter-laboratory and inter-habitat comparisons. To address this we recommend that  
543 reference material be produced and distributed between laboratories.

544  
545 **Nitrous oxide:** Some of the trends discussed for methane were also evident in the nitrous oxide  
546 data. For the samples with the lowest nitrous oxide concentrations a skewed data distribution  
547 was observed, as found for methane (Fig. 4c). Such low nitrous oxide concentrations are typical  
548 of low-oxygen water-column environments (<10 μmol kg<sup>-1</sup>). Therefore, the analytical bias  
549 towards measuring values higher than the absolute *in situ* concentrations is particularly pertinent  
550 to oceanographers measuring nitrous oxide in oxygen minimum zones and other low-oxygen  
551 environments (Naqvi et al., 2010; Farías et al., 2015; Ji et al., 2015). The low concentrations of  
552 nitrous oxide still exceed detection limits by at least an order of magnitude for even the less-  
553 sensitive headspace method due to the high sensitivity of the ECD. Therefore, the bias towards  
554 reporting elevated values for low concentrations of nitrous oxide is related less to analytical  
555 sensitivity and is more a consequence of calibration issues. During the intercomparison exercise  
556 ECD calibration was identified as a nontrivial issue for all participating laboratories and it  
557 deserves continuing attention. In particular, the nonlinearity of the ECD means that low and

558 high nitrous oxide concentrations are more vulnerable to error since the values fall outside of the  
559 most frequented part of the calibration curve. This is particularly true if a linear fit is used to  
560 calibrate the ECD (Fig. 6a). To circumvent this problem, one laboratory used a step-wise linear  
561 function while other laboratories used a quadratic function. The usefulness of multiple  
562 calibration curves for low and high nitrous oxide concentrations was highlighted during the  
563 intercomparison exercise, although this necessitates some consideration of the threshold for  
564 switching **between** different calibration curves.

565 The majority of seawater samples analyzed had nitrous oxide concentrations ranging from 7–  
566 11 nmol kg<sup>-1</sup> (Fig. 4a, 4b), which are close to atmospheric equilibrium values, as shown for the  
567 Pacific Ocean (Fig. 4b). Collective analysis of these samples gives insight into the precision and  
568 accuracy associated with surface water nitrous oxide analysis (Fig 5a). This is discussed further  
569 in the context of implementing internal controls for methane and nitrous oxide (Section 4.4). For  
570 samples with the highest nitrous oxide concentrations, *i.e.* exceeding 30 nmol kg<sup>-1</sup>, there was  
571 high variability between the concentrations reported by the independent laboratories. This was  
572 most evident for the BAL5 samples (Fig. 4e) and similar to the variability observed at the highest  
573 methane concentrations analyzed (Fig. 1e). It is difficult to assess how much of this variability  
574 was specifically due to the differences in calibration practices between the laboratories and the  
575 differences in gas standards with high nitrous oxide mole fractions, but at least some of it can be  
576 attributed to this. These results form the basis for a proposed production of reference material  
577 for both trace gases.

578

### 579 **4.3 Are there general recommendations to reduce uncertainty in the accuracy and** 580 **precision of methane and nitrous oxide measurements?**

581 **There are several analytical recommendations resulting from this study. The use of highly**  
582 **accurate standards and the appropriate calibration fit is an essential requirement for both**  
583 **headspace equilibration and the purge-and-trap technique. It was shown that both analytical**  
584 **approaches can yield comparable values for methane and nitrous oxide, with the main**  
585 **differences observed at low methane concentrations. At sub-nanomolar methane concentrations,**  
586 **four out of the six laboratories that reported methane concentrations <1 nmol kg<sup>-1</sup> used a purge-**  
587 **and-trap analysis.**

588 This study also revealed that sample storage time can be an important factor. Specifically,  
589 the results from this study corroborate the findings of Magen et al. (2014) who showed that  
590 samples with low concentrations of methane and more susceptible to increased values as a result  
591 of contamination. The contamination was most likely due to the release of methane and other  
592 hydrocarbons from the septa (Niemann et al., 2015). Since the release of hydrocarbons occurs  
593 over a period of time, it is recommended to keep storage time to a minimum and to store samples  
594 in the dark. It should be noted that sample integrity can also be compromised due to other  
595 factors including inadequate preservation, outgassing, and adsorption of gases onto septa. For all  
596 these reasons, it is recommended to conduct an evaluation of sample storage time for the  
597 environment that is being sampled.

598 One useful item that was not included as part of the intercomparison exercise but can help  
599 decrease uncertainty in the accuracy and precision of methane and nitrous oxide measurements  
600 are internal control measurements. Internal controls represent a self-assessment quality control  
601 check to validate the analytical method and quantify the magnitude of uncertainty. Appropriate  
602 internal controls for methane and nitrous oxide consist of air-equilibrated seawater samples.  
603 Their purpose is to provide checks for methane concentrations ranging from 2–3 nmol kg<sup>-1</sup> and  
604 for nitrous oxide concentrations from 5–9 nmol kg<sup>-1</sup>. The air used in the equilibration process  
605 could be sourced from the ambient environment if sufficiently stable or from a compressed gas  
606 cylinder after cross-checking the concentration with the appropriate gas standard. Air-  
607 equilibrated samples provide reassurance that the analytical system is providing values within the  
608 correct range. Air-equilibrated samples also indicate the certainty associated with calculating the  
609 saturation state of the ocean with respect to atmospheric equilibrium. This is particularly  
610 relevant when the seawater being sampled is within a few percent of saturation. Finally, these  
611 air-equilibrated samples provide an estimate of analytical accuracy, which is infrequently  
612 reported for methane or nitrous oxide. At present, only a few studies report the analysis of air-  
613 equilibrated seawater alongside water-column samples (Bullister and Wisegarver, 2008; Capelle  
614 et al., 2015; Bourbonnais et al., 2017; Wilson et al., 2017). It is likely that wider implementation  
615 would facilitate internal assessment of the analytical system. Since the main equipment required  
616 is a water-bath and an overhead stirrer, the production is not cost-prohibitive. A  
617 recommendation of this intercomparison exercise is that laboratories routinely use air-  
618 equilibrated seawater samples to provide an estimate of analytical accuracy.

619 In addition to the self-assessments provided by the analysis of air-equilibrated seawater, this  
620 study revealed the need for reference seawater to help assess the accuracy of high concentration  
621 methane and nitrous oxide measurements. Reference seawater in this instance refers to batches  
622 of dissolved methane and nitrous oxide samples prepared in the laboratory using an equilibrator  
623 set-up, as used for dissolved inorganic carbon (Dickson et al., 2007). In the absence of plans for  
624 additional intercomparison exercises, the provision of reference seawater will allow laboratories  
625 to continue evaluating their own measurements. **Finally, the lessons learned during the**  
626 **intercomparison exercises will be the basis for a forthcoming Good Practice Guide for dissolved**  
627 **methane and nitrous oxide.**

628

#### 629 **4.4 What are the implications of interlaboratory differences for determining the spatial and** 630 **temporal variability of methane and nitrous oxide in the oceans?**

631 The key outcome of this study was the identification of differences in methane and nitrous oxide  
632 concentrations for the same batch of seawater samples measured by several independent  
633 laboratories. Emergent from this is the distinct possibility that any given laboratory will  
634 incorrectly report data, thereby increasing uncertainty over the saturation states of both gases.  
635 The tendency to over-estimate methane concentrations close to atmospheric equilibrium means  
636 that marine emissions of methane to the overlying atmosphere will be also overestimated (Bange  
637 et al., 1994; Upstill-Goddard and Barnes, 2016). In contrast, for nitrous oxide there does not  
638 appear to be either an under-estimation or over-estimation of concentrations. Consequently, there  
639 is generally a lower inherent uncertainty in its surface ocean saturation state, as previously  
640 proposed (Law and Ling, 2001; Forster et al., 2009).

641 The inter-laboratory differences highlighted by this study should be viewed in the context of  
642 numerous individual efforts to assess temporal and/or spatial trends in methane and nitrous oxide  
643 by way of time-series observations (Bange et al., 2010; Farías et al., 2015; Wilson et al., 2017;  
644 Fenwick and Tortell, 2018), repeat hydrographic survey lines (de la Paz et al., 2017), and single  
645 expeditions. While the value of these in integrating the behaviour of methane and nitrous oxide  
646 into the hydrography and biogeochemistry of local-regional ecosystems is beyond question, their  
647 value would be enhanced by the rigorous cross-validation of analytical protocols. Without this,  
648 perceived small temporal and/or spatial changes in water-column concentrations in any given  
649 region are difficult to verify unless the data all originate from a single laboratory. In addition,

650 the value of a global methane and nitrous oxide database (*e.g* Bange et al., 2009) would to some  
651 extent be compromised by the uncertainty. Taking due account of the analytical variability  
652 between laboratories will clearly be vital to any future assessment of the changing methane and  
653 nitrous oxide budgets of the oceans.

654

## 655 **5. Conclusions**

656 Overall, the intercomparison exercise was invaluable to the growing community of ocean  
657 scientists interested in understanding the dynamics of dissolved methane and nitrous oxide in the  
658 water-column. The level of agreement between independent measurements of dissolved  
659 concentrations was evaluated in the context of several contributing factors, including sample  
660 analysis, standards, calibration procedures, and sample storage time. Importantly, the  
661 intercomparison represents a concerted effort from the scientists involved to critically assess the  
662 quality of their data, and to initiate the steps required for further improvements.

663 Recommendations arising from the intercomparison include routine cross-calibration of working  
664 gas standards against primary standards, minimizing sample storage time, incorporating internal  
665 controls (air-equilibrated seawater) alongside routine sample analysis, and the future production  
666 of reference seawater for methane and nitrous oxide measurements. These efforts will help  
667 resolve temporal and spatial variability, which is necessary for constraining methane and nitrous  
668 oxide emissions from aquatic ecosystems and for evaluating the processes that govern their  
669 production and consumption in the water-column.

670 *Acknowledgements:*

671 **During the final stages of this work, our coauthor John Bullister passed away. The**  
672 **intercomparison exercise greatly benefited from John's scientific expertise on dissolved gases.**  
673 **He will be greatly missed by the oceanographic community.**

674 The methane and nitrous oxide intercomparison exercise was conducted as a Scientific  
675 Committee on Ocean Research (SCOR) Working Group which receives funding from the U.S.  
676 National Science Foundation (OCE-1546580). Pacific Ocean seawater samples were collected  
677 on HOT cruises which are supported by NSF (including the most recent OCE-1260164 to  
678 DMK). Baltic Sea seawater samples were collected during Cruise #142 of the RV *Elisabeth*  
679 *Mann Borgese*, with the ship-time provided by the Leibniz Institute for Baltic Sea Research  
680 Warnemünde. We thank Ligu Guo for help with sampling during the Baltic Sea cruise. The  
681 methane and nitrous oxide gas standards were produced via a Memorandum of Understanding  
682 between the University of Hawai'i and NOAA-PMEL. Funding for the gas standards was  
683 provided by for the Center for Microbial Oceanography: Research and Education (C-MORE;  
684 EF0424599 to DMK), SCOR, the EU FP7 funded Integrated non-CO<sub>2</sub> Greenhouse gas  
685 Observation System (InGOS) (Grant Agreement #284274), and NOAA's Climate Program  
686 Office, Climate Observations Division. Additional support was provided by the Gordon and  
687 Betty Moore Foundation #3794 (DMK), the Simons Collaboration on Ocean Processes and  
688 Ecology (SCOPE; #329108 to DMK), and the Global Research Laboratory Program (#  
689 2013K1A1A2A02078278 to DMK) through the National Research Foundation of Korea (NRF).  
690 AVB is a senior research associate at the FRS-FNRS. AES would like to acknowledge NSF  
691 OCE-1437310. MP would like to acknowledge the support of the Spanish Ministry of Economy  
692 and Competitiveness (CTM2015-74510-JIN). LF received financial support by FONDAP  
693 1511009 and FONDECYT N°1161138. Any use of trade names is for descriptive purposes and  
694 does not imply endorsement by the U.S. government



695 **References**

- 696 Anderson, B., Bartlett, K., Frolking, S., Hayhoe, K., Jenkins, J., and Salas, W.: Methane and  
697 nitrous oxide emissions from natural sources, Office of Atmospheric Programs, US EPA,  
698 EPA 430-R-10-001, Washington DC, 2010.
- 699 Arévalo-Martínez, D. L., Beyer, M., Krumbholz, M., Piller, I., Kock, A., Steinhoff, T.,  
700 Körtzinger, A., and Bange, H. W.: A new method for continuous measurements of oceanic  
701 and atmospheric N<sub>2</sub>O, CO and CO<sub>2</sub>: performance of off-axis integrated cavity output  
702 spectroscopy (OA-ICOS) coupled to non-dispersive infrared detection (NDIR), *Ocean Sci.*,  
703 9, 1071–1087, 2013.
- 704 Atkinson, L. P., and Richards, F. A.: The occurrence and distribution of methane in the marine  
705 environment, *Deep-Sea Res.*, 14, 673–684, 1967.
- 706 Bange, H. W., Bartell, U. H., Rapsomanikis, S., and Andreae, M. O.: Methane in the Baltic and  
707 North Seas and a reassessment of the marine emissions of methane, *Global Biogeochem.*  
708 *Cycles*, 8, 465–480, doi:10.1029/94GB02181, 1994.
- 709 Bange, H. W., Rapsomanikis, S., and Andreae, M. O.: Nitrous oxide cycling in the Arabian Sea,  
710 *J. Geophys. Res.: Oceans*, 106, 1053–1065, 2001.
- 711 Bange H.W, Bell, T.G., Cornejo, M., Freing, A., Uher, G., Upstill-Goddard, R.C., and Zhang G.  
712 MEMENTO: a proposal to develop a database of marine nitrous oxide and methane  
713 measurements. *Env. Chem*, 6, 195–197, 2009.
- 714 Bange, H.W., Bergmann, K., Hansen, H.P., Kock, A., Koppe, R., Malien, F., and Ostrau, C.:  
715 Dissolved methane during hypoxic events at the Boknis Eck Time Series Station  
716 (Eckernförde Bay, SW Baltic Sea), *Biogeosciences.*, 7, 1279–1284, 2010.
- 717 Borges, A.V., Speeckaert, G., Champenois, W., Scranton, M.I., and Gypens, N.: Productivity and  
718 temperature as drivers of seasonal and spatial variations of dissolved methane in the Southern  
719 Bight of the North Sea, *Ecosystems*, 1–17, 2017.
- 720 Bourbonnais, A., Letscher, R. T., Bange, H. W., Échevin, V., Larkum, J., Mohn, J., N. Yoshida,  
721 N., and Altabet, M. A.: N<sub>2</sub>O production and consumption from stable isotopic and  
722 concentration data in the Peruvian coastal upwelling system, *Global Biogeochem. Cycles*, 31,  
723 678–698, 2017. doi:10.1002/2016GB005567.
- 724 Bullister, J. L., and Wisegarver, D. P.: The shipboard analysis of trace levels of sulfur  
725 hexafluoride, chlorofluorocarbon-11 and chlorofluorocarbon-12 in seawater, *Deep-Sea Res.*,  
726 55, 1063–1074, 2008.

727 Bullister, J. L., and Tanhua, T.: Sampling and measurement of chlorofluorocarbons and sulfur  
728 hexafluoride in seawater, IOCCP Report No. 14 ICPO Publication Series No. 134, Version 1,  
729 2010.

730 Bullister, J. L., Wisegarver, D. P., and Wilson, S. T.: The production of methane and nitrous  
731 oxide gas standards for Scientific Committee on Ocean Research (SCOR) Working Group  
732 #143, <http://udspace.udel.edu/handle/19716/23288>, 2016.

733 Bussmann, I., Matousu, A., Osudar, R. and Mau, S.: Assessment of the radio  $^3\text{H-CH}_4$  tracer  
734 technique to measure aerobic methane oxidation in the water column, *Limnol. Oceanogr.:*  
735 *Methods*, 13, 312–327, 2015.

736 Butler, J. H., Elkins, J. W., Thompson, T. M., and Egan, K. B.: Tropospheric and dissolved  $\text{N}_2\text{O}$   
737 of the west Pacific and east Indian Oceans during the El Niño Southern Oscillation Event of  
738 1987, *J. Geophys. Res.*, 94, 14,865–14,877, 1989.

739 Butler, J. H., and Elkins, J. W.: An automated technique for the measurement of dissolved  $\text{N}_2\text{O}$   
740 in natural waters, *Mar. Chem.*, 34, 47–61, 1991.

741 Capelle, D. W., Dacey, J. W., and Tortell, P. D.: An automated, high through-put method for  
742 accurate and precise measurements of dissolved nitrous oxide and methane concentrations in  
743 natural waters, *Limnol. Oceanogr.:* *Methods*, 13, 345–355, 2015.

744 Ciais, P., Dolman, A.J., Bombelli, A., Duren, R., Pregon, A., Rayner, P.J., Miller, C., Gobron,  
745 N., Kinderman, G., Marland, G., and Gruber, N.: Current systematic carbon-cycle  
746 observations and the need for implementing a policy-relevant carbon observing system,  
747 *Biogeosciences*, 11, 3547–3602, 2014.

748 Craig, H. and Gordon, L. I.: Nitrous oxide in the ocean and the marine atmosphere, *Geochim.*  
749 *Cosmochim. Acta* 27, 949–955, 1963.

750 Cutter, G. A.: Intercalibration in chemical oceanography - getting the right number. *Limnol.*  
751 *Oceanogr.:* *Methods*, 11, 418–424, 2013.

752 de la Paz, M., García-Ibáñez, M.I., Steinfeldt, R., Ríos, A.F., and Pérez, F.F.: Ventilation versus  
753 biology: What is the controlling mechanism of nitrous oxide distribution in the North  
754 Atlantic?, *Global Biogeochem. Cycles*, 31, 745–760, doi: 10.1002/2016GB005507, 2017.

755 Dickson, A. G., Sabine, C. L. and Christian, J. R.: Guide to best practices for ocean  $\text{CO}_2$   
756 measurements, PICES Special Publication 3, 2007.

757 Farías, L., Castro-González, M., Cornejo, M., Charpentier, J., Faúndez, J., Boontanon, N. and  
758 Yoshida, N.: Denitrification and nitrous oxide cycling within the upper oxycline of the

759 eastern tropical South Pacific oxygen minimum zone. *Limnol. Oceanogr.*, 54, 132–144,  
760 2009.

761 Farías, L., Besoain, V., and García-Loyola, S.: Presence of nitrous oxide hotspots in the coastal  
762 upwelling area off central Chile: an analysis of temporal variability based on ten years of a  
763 biogeochemical time series, *Environ. Res. Lett.*, 10, 044017, 2015.

764 Fenwick, L., and Tortell, P. D.: Methane and nitrous oxide distributions in coastal and open  
765 ocean waters of the Northeast Subarctic Pacific during 2015–2016, *Mar. Chem.*, 200, 45–56,  
766 2018.

767 Fenwick, L., Capelle, D., Damm, E., Zimmermann, S., Williams, W. J., Vagle, S., and Tortell, P.  
768 D.: Methane and nitrous oxide distributions across the North American Arctic Ocean during  
769 summer, 2015, *J. Geophys. Res.: Oceans*, 122, 390–412, doi:10.1002/2016JC012493, 2017.

770 Forster, G., Upstill-Goddard, R. C., Gist, N., Robinson, C., Uher, G. and Woodward, E. M. S.:  
771 Nitrous oxide and methane in the Atlantic Ocean between 50 N and 52 S: latitudinal  
772 distribution and sea-to-air flux, *Deep-Sea Res.*, 56, 964–976, 2009.

773 Freing, A., Wallace, D. W. R., and Bange, H. W.: Global oceanic production of nitrous oxide,  
774 *Phil. Trans. R. Soc. B*, 367, 1245–1255, 2012.

775 Gülzow, W., Rehder, G., Schneider, B., Schneider, J., Deimling, V., and Sadkowiak, B.: A new  
776 method for continuous measurement of methane and carbon dioxide in surface waters using  
777 off-axis integrated cavity output spectroscopy (ICOS): An example from the Baltic Sea,  
778 *Limnol. Oceanogr.: Methods*, 9, 176–184, 2011.

779 Jakobs, G., Holterman, P., Berndmeyer, C., Rehder, G., Blumenberg, M., Jost, G., Nausch, G.,  
780 and Schmale, O.: Seasonal and spatial methane dynamics in the water column of the central  
781 Baltic Sea (Gotland Sea), *Cont. Shelf Res.*, 91, 12–25, 2014.

782 Ji, Q., Babbín, A. R., Jayakumar, A., Oleynik, S., and Ward, B. B.: Nitrous oxide production by  
783 nitrification and denitrification in the Eastern Tropical South Pacific oxygen minimum zone,  
784 *Geophys. Res. Lett.*, 42, 10,755–10,764, doi:10.1002/2015GL066853, 2015.

785 Kitidis, A., Upstill-Goddard, R. C., and Anderson, L. G.: Methane and nitrous oxide in surface  
786 water along the North-West Passage, Arctic Ocean, *Mar. Chem.*, 121, 80–86, 2010.

787 Law, C. S., and Ling, R. D.: Nitrous oxide flux and response to increased iron availability in the  
788 Antarctic Circumpolar Current, *Deep-Sea Res.*, 48, 2509–2527, 2001.

789 Magen, C., Lapham, L. L., Pohlman, J. W., Marshall, K., Bosman, S., Casso, M., and Chanton, J.  
790 P.: A simple headspace equilibration method for measuring dissolved methane, *Limnol.*  
791 *Oceanogr.: Methods*, 12, 637–650, 2014.

- 792 McAuliffe, C.: Solubility on water of C<sub>1</sub>-C<sub>9</sub> hydrocarbons, *Nature*, 200, 1092–1093, 1963.
- 793 Myhre, G., Shindell, D., Bréon, F.-M., Collins, W., Fuglestedt, J., Huang, J., Koch, D.,  
794 Lamarque, J.-F., Lee, D., Mendoza, B., Nakajima, T., Robock, A., Stephens, G., Takemura,  
795 T., and Zhang, H.: Anthropogenic and Natural Radiative Forcing, In: *Climate Change 2013:  
796 The Physical Science Basis. Contribution of Working Group I to the Fifth Assessment Report  
797 of the Intergovernmental Panel on Climate Change* [Stocker, T. F., Qin, D., Plattner, G.-K.,  
798 Tignor, M., Allen, S. K., Boschung, J., Nauels, A., Xia, Y., Bex, V., and Midgley, P. M.  
799 (eds.)]. Cambridge University Press, Cambridge, United Kingdom and New York, NY, USA,  
800 2013.
- 801 Naqvi, S. W. A., Bange, H. W., Farías, L., Monteiro, P. M. S., Scranton, M. I., and Zhang, J.:  
802 Marine hypoxia/anoxia as a source of CH<sub>4</sub> and N<sub>2</sub>O, *Biogeosciences*, 7, 215–2190, doi:  
803 10.5194/bg-7-2159-2010, 2010.
- 804 National Research Council: *Applications of analytical chemistry to oceanic carbon cycle studies.*  
805 Washington DC. National Academy Press, 1993.
- 806 Nevison, C. D., Weiss, R. F., and Erickson, D. J.: Global oceanic emissions of nitrous oxide, *J.*  
807 *Geophys. Res.*, 100, 15809–15820, doi: 10.1029/95JC00684, 1995.
- 808 Niemann, H., Steinle, L., Brees, J., Bussmann, I., Treude, T., Krause, S., Elvert, M., and  
809 Lehmann, M. F.: Toxic effects of lab-grade butyl rubber stoppers on aerobic methane  
810 oxidation, *Limnol. Oceanogr.: Methods*, 13, 40–52, 2015.
- 811 Pohlman, J. W., Bauer, J. E., Waite, W. F., Osburn, C. L., and Chapman, N. R.: Methane  
812 hydrate-bearing seeps as a source of aged dissolved organic carbon to the oceans, *Nature*  
813 *Geosci.*, 4, 37–41, 2011.
- 814 Reeburgh, W. S.: Oceanic methane biogeochemistry, *Chem. Rev.*, 107, 486–513, doi:  
815 10.1021/cr050362v, 2007.
- 816 Rehder, G., Keir, R. S., Suess, E., and Rhein, M.: Methane in the northern Atlantic controlled by  
817 microbial oxidation and atmospheric history, *Geophys. Res. Lett.*, 26, 587–590, doi:  
818 10.1029/1999GL900049, 1999.
- 819 Schmale, O., Schneider von Deimling, J., Gülzow, W., Nausch, G., Waniek, J. J. and Rehder, G.:  
820 Distribution of methane in the water column of the Baltic Sea. *Geophys. Res. Lett.*, 37,  
821 L12604, doi: 10.1029/2010GL043115, 2010.
- 822 Strady, E., Pohl, C., Yakushev, E. V., Krügera, S., and Hennings, U.: PUMP–CTD-System for  
823 trace metal sampling with a high vertical resolution. A test in the Gotland Basin, Baltic Sea,  
824 *Chemosphere*, 70, 1309–1319, 2008.

- 825 Swan, H. B., Armishaw, P., Iavetz, R., Alamgir, M., Davies, S. R., Bell, T. G., and Jones, G. B.:  
826 An interlaboratory comparison for the quantification of aqueous dimethylsulfide. *Limnol.*  
827 *Oceanogr.: Methods*, 12, 784–794, 2014.
- 828 Upstill-Goddard, R. C., Rees, A. P., and Owens, N. J. P.: Simultaneous high-precision  
829 measurements of methane and nitrous oxide in water and seawater by single phase  
830 equilibration gas chromatography, *Deep-Sea Res.*, 43, 1669–1682, 1996.
- 831 Upstill-Goddard, R. C., and Barnes, J.: Methane emissions from UK estuaries: Re-evaluating the  
832 estuarine source of tropospheric methane from Europe, *Mar. Chem.*, 180, 14–23, 2016.
- 833 Walter, S., Peeken, I., Lochte, K., Webb, A., and Bange, H. W.: Nitrous oxide measurements  
834 during EIFEX, the European Iron Fertilization Experiment in the subpolar South Atlantic  
835 Ocean, *Geophys. Res. Lett.*, 32, doi:10.1029/2005GL024619, 2005.
- 836 Weiss, R. F., and Price, B. A.: Nitrous oxide solubility in water and seawater, *Mar. Chem.*, 8,  
837 347–359, doi: 10.1016/0304-4203(80)90024-9, 1980.
- 838 Weiss, R. F., Van Woy, F. A., and Salameh, P. K.: Surface water and atmospheric carbon  
839 dioxide and nitrous oxide observation by shipboard automated gas chromatography: Results  
840 from expeditions between 1977 and 1990, Scripps Institution of oceanography Reference 92-  
841 11. ORNL/CDIAC-59, NDP-044. Carbon Dioxide Information Analysis Center, Oak Ridge  
842 National Laboratory, Tennessee, 1992.
- 843 Wiesenburg, D. A., and Guinasso, N. L.: Equilibrium solubilities of methane, carbon monoxide  
844 and hydrogen in water and seawater, *J. Chem. Eng. Data*, 24, 354–360, doi:  
845 10.1021/je60083a006, 1979.
- 846 Wilson, S. T., Ferrón, S., and Karl, D. M.: Interannual variability of methane and nitrous oxide in  
847 the North Pacific Subtropical Gyre, *Geophys. Res. Lett.*, 44, doi: 10.1002/2017GL074458,  
848 2017.
- 849 Zhang, G. L., Zhang, J., Kang, Y. B., and Liu, S. M.: Distributions and fluxes of methane in the  
850 East China Sea and the Yellow Sea in spring, *J. Geophys. Res.*, 109, C07011,  
851 doi:10.1029/2004JC002268, 2004

852 **Table 1.** List of laboratories that participated in the intercomparison. All laboratories measured  
 853 both methane and nitrous oxide except U.S. Geological Survey (methane only), U.C. Santa  
 854 Barbara (nitrous oxide only), and NOAA PMEL (nitrous oxide from the Pacific Ocean). Also  
 855 indicated are the twelve laboratories that received the SCOR gas standards of methane and  
 856 nitrous oxide.

<b>Institution</b>	<b>Lead Scientist</b>	<b>SCOR Standards</b>
University of Hawai'i, USA	Samuel Wilson	Yes
GEOMAR, Germany	Hermann Bange	Yes
Newcastle University, UK	Robert Upstill-Goddard	Yes
Université de Liège, Belgium	Alberto Vieira Borges	No
Plymouth Marine Laboratory, UK	Andrew Rees	Yes
NOAA PMEL, USA	John Bullister	Yes
IIM-CSIC, Spain	Mercedes de la Paz	Yes
CACYTMAR, Spain	Macarena Burgos	No
University of Concepción, Chile	Laura Farías	Yes
IOW, Germany	Gregor Rehder	Yes
University of California Santa Barbara, USA	Alyson Santoro	Yes
National Institute of Water and Atmospheric Research, NZ	Cliff Law	Yes
University British Columbia, Canada	Philippe Tortell	Yes
U.S. Geological Survey, USA	John Pohlman	No
Ocean University of China, China	Guiling Zhang	Yes

857

858

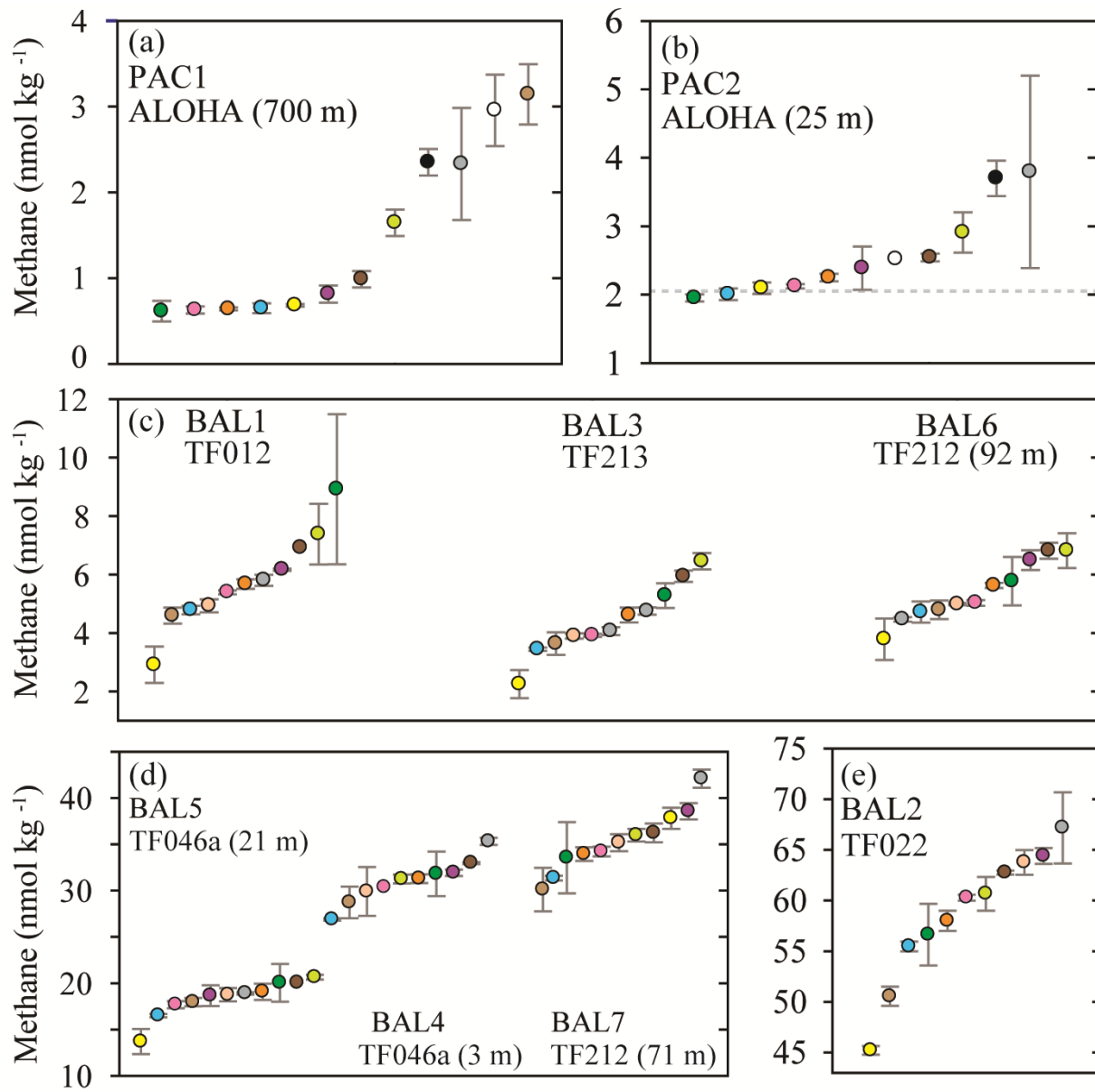
859 **Table 2.** Pertinent information for each batch of methane and nitrous oxide samples. This  
 860 includes contextual hydrographic information, median and mean concentrations of methane and  
 861 nitrous oxide, range, number of outliers, and the overall average coefficient of variation (%).  
 862

<b>Sampling parameters</b>									
Sample ID	PAC1	PAC 2	BAL1	BAL2	BAL3	BAL4	BAL5	BAL6	BAL7
Location	22.75N 158.00W	22.75N 158.00W	54.32N 11.55E	54.11N 11.18E	55.25N 15.98E	55.30N 15.80E	55.30N 15.80E	54.47N 12.21E	54.47N 12.21E
Location name	Station ALOHA	Station ALOHA	TF012	TF022	TF213	TF212	TF212	TF046a	TF046a
Sampling date	24.2.17	24.2.17	16.10.16	17.10.16	18.10.16	19.10.16	20.10.16	21.10.16	21.10.16
Sampling depth (m)	25	700	3	22	3	92	71	3	21
Seawater temperature (°C)	23.6	5.1	12.0	13.6	12.2	6.6	6.7	11.8	13.4
Salinity	34.97	34.23	13.85	17.37	7.87	18.40	18.08	8.81	17.65
Density (kg m <sup>-3</sup> )	1024	1027	1010	1013	1006	1014	1014	1006	1013
<b>Nitrous oxide</b>									
Number of datasets	13	13	12	13	12	13	12	13	12
Outliers	0	1	2	1	1	0	1	2	2
Median N <sub>2</sub> O conc. (nmol kg <sup>-1</sup> )	42.4	7.0	11.0	9.4	11.1	3.4	40.2	11.0	9.6
Mean N <sub>2</sub> O conc. (nmol kg <sup>-1</sup> )	41.3	7.0	11.1	9.2	11.0	3.4	39.0	10.8	9.5
Range	34.3-45.8	5.9-7.6	10.1-12.7	7.7-11.0	9.6-11.6	2.1-5.5	30.1-45.9	9.5-11.5	8.0-10.4
Average coeff. variation (%)	2.8	4.4	4.5	4.2	2.7	7.5	4.0	2.6	4.4
<b>Methane</b>									
Number of datasets	12	12	11	11	11	11	11	11	11
Outliers	0	1	0	0	0	1	1	0	0
Median CH <sub>4</sub> conc. (nmol kg <sup>-1</sup> )	0.9	2.3	5.7	60.3	4.1	31.3	18.8	5.0	35.2
Mean CH <sub>4</sub> conc. (nmol kg <sup>-1</sup> )	1.8	2.6	5.8	58.6	4.4	31.1	18.8	5.4	35.4
Range	0.6-3.1	1.9-3.8	2.9-8.9	45.2-67.2	2.5-6.5	26.9-35.3	16.5-20.7	3.8-6.8	30.1-42.1
Average coeff. variation (%)	10.9	7.2	8.6	2.1	4.3	3.5	4.2	6.5	3.5

863

864

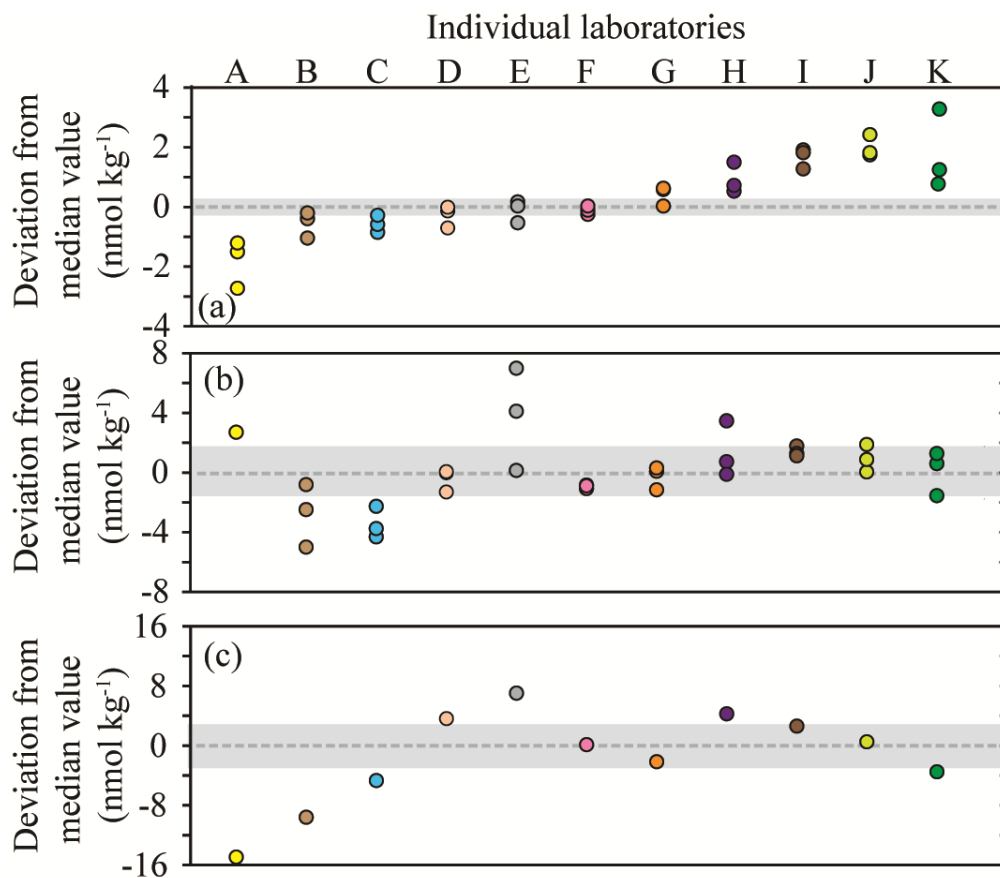
865 **Figures**



866  
 867  
 868 Figure 1. Concentrations of methane measured in nine separate seawater samples collected from  
 869 the Pacific Ocean (Fig. 1a, 1b) and the Baltic Sea (Fig. 1c, 1d, 1e). The dashed grey line  
 870 represents the value of methane at atmospheric equilibrium (Fig. 1b.) Individual data points are  
 871 plotted sequentially by increasing value. The same color symbol is used for each laboratory in  
 872 all plots.

873  
 874

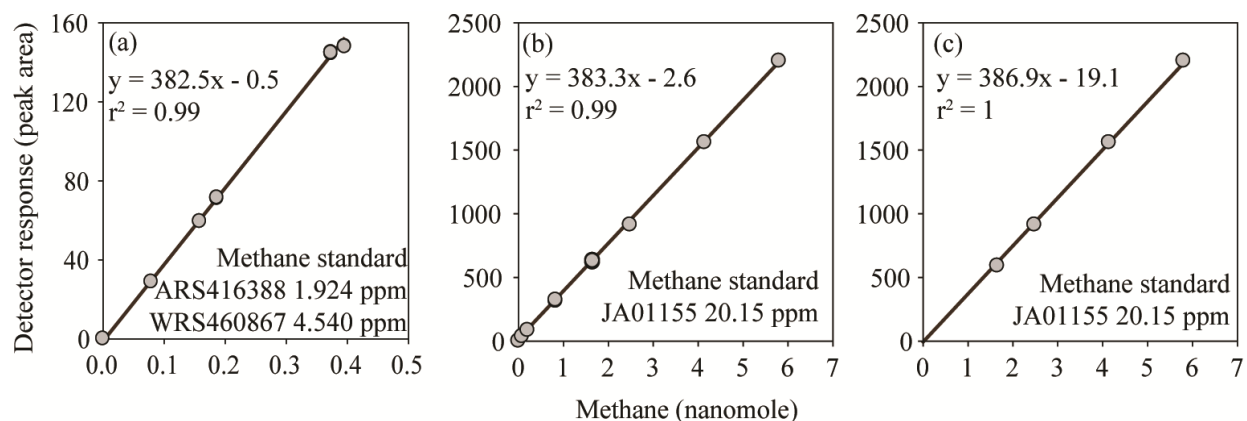




875  
 876 Figure 2. Deviation from the median methane concentration (reported as absolute values in nmol  
 877  $\text{kg}^{-1}$ ) for the seven Baltic Sea samples. The batches of seawater samples include BAL1, BAL3,  
 878 and BAL6 (Fig. 2a), BAL4, BAL5, and BAL7 (Fig. 2b), and BAL2 (Fig. 2c). The shaded grey  
 879 area indicates values  $\leq 5\%$  of the median concentration. The color scheme for each laboratory  
 880 dataset is identical to that used in Figure 1 and the letters allocated to each dataset are to facilitate  
 881 cross-referencing in the text. Note that the y-axis scale varies between the Figures.

882

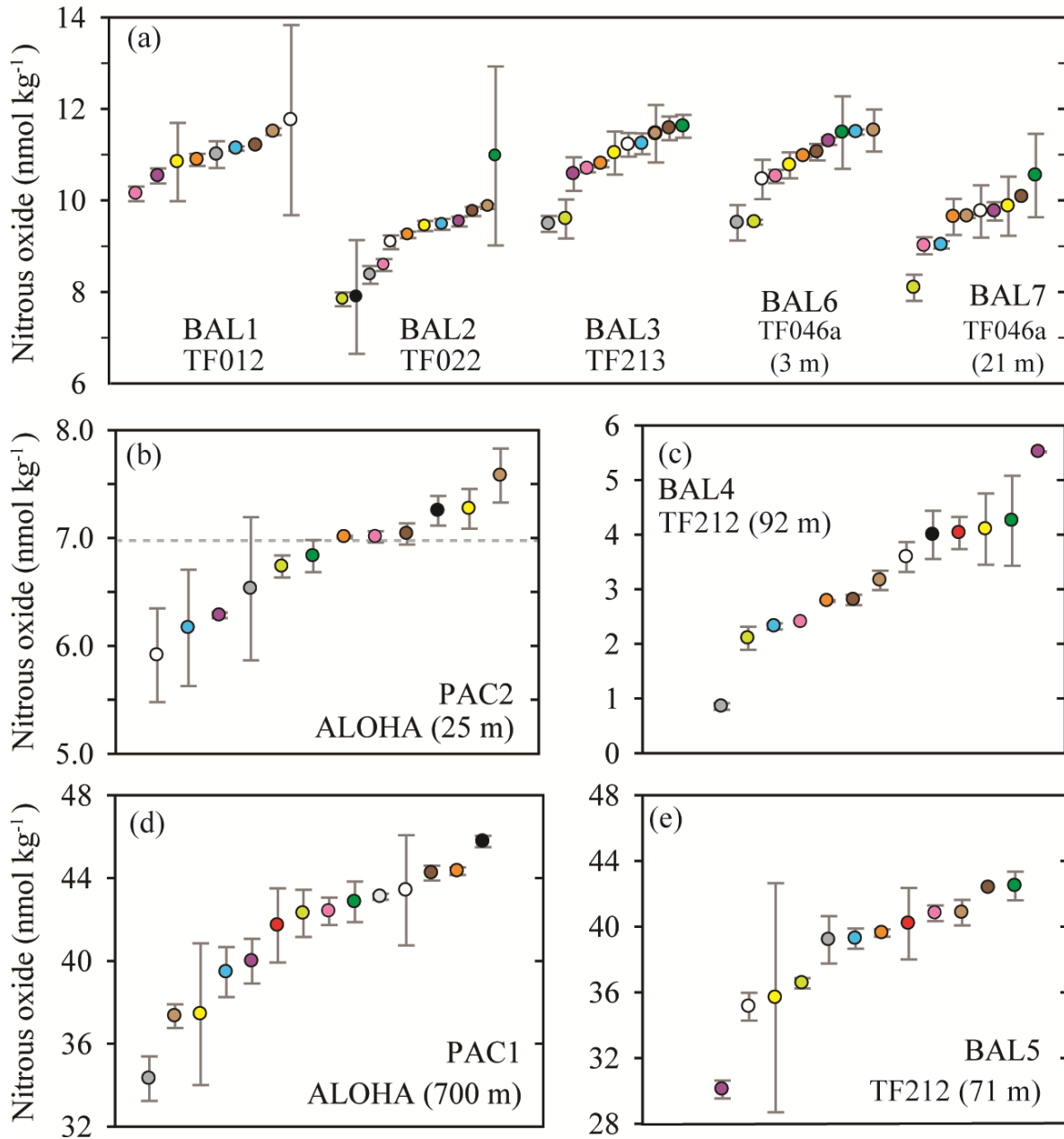
883



884

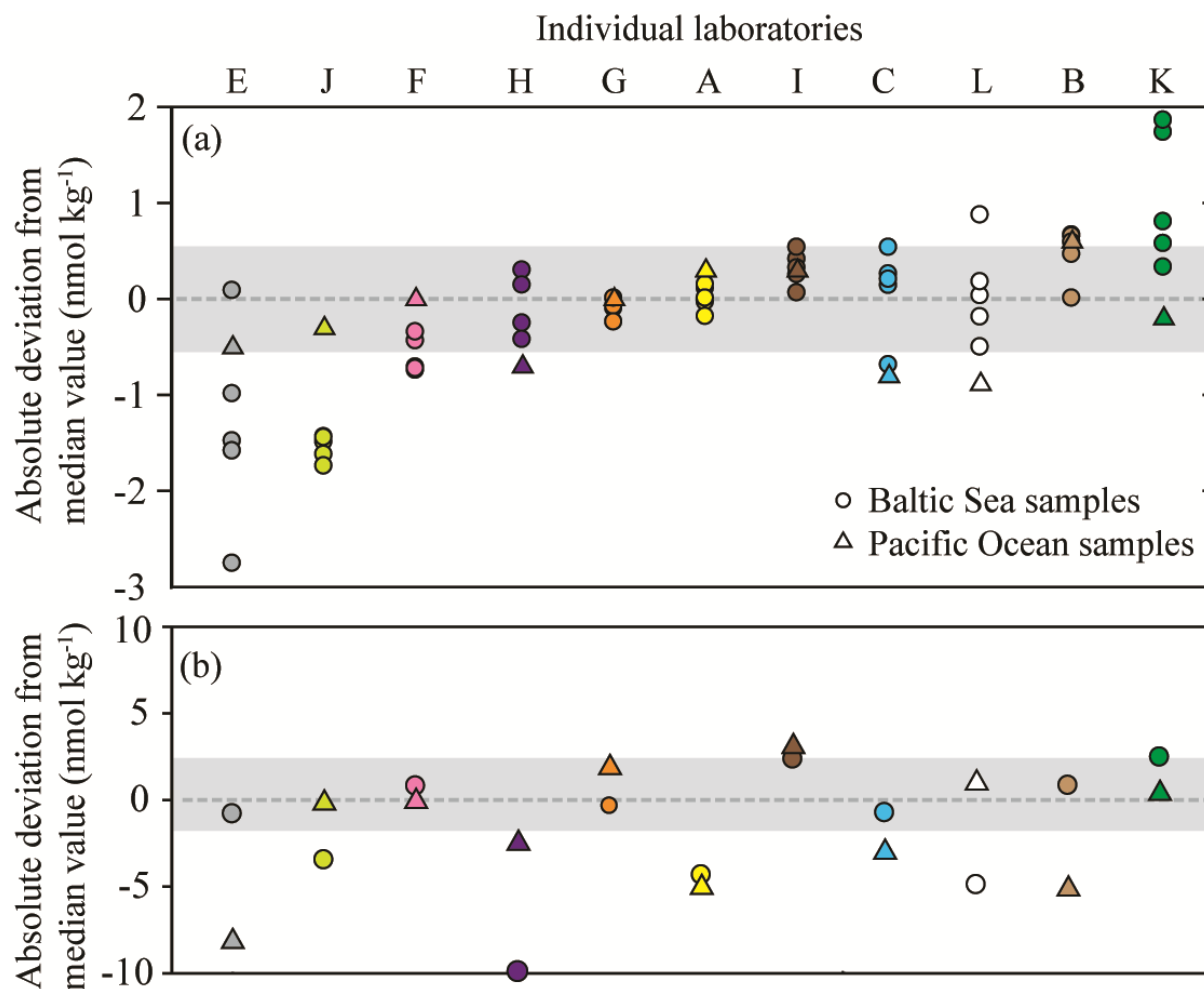
885 Figure 3. FID response to methane, fitted with a linear regression calibration. The inclusion  
886 (Fig. 3a and Fig. 3b) or exclusion (Fig. 3c) of low methane values cause the calibration slope and  
887 intercept to vary. However, the observed variation in the calibration slope does not have a  
888 significant effect on the final calculated concentrations of methane. In contrast, variation in the  
889 intercept does have an effect on the final concentrations of methane.

890



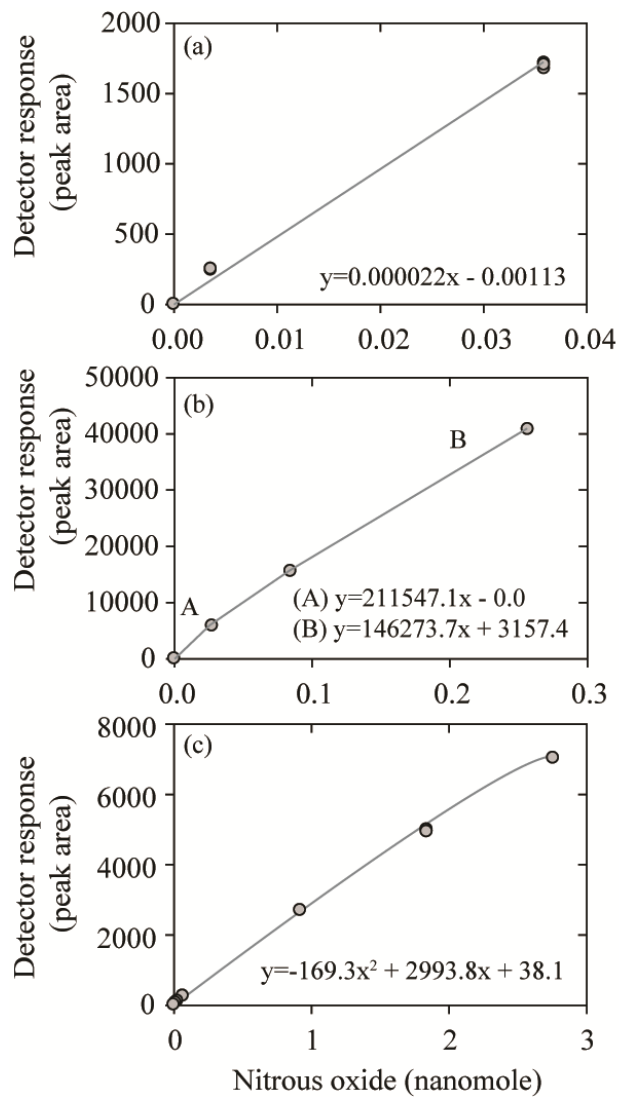
891  
 892  
 893  
 894  
 895  
 896  
 897

Figure 4. Concentrations of nitrous oxide measured in nine separate samples from the Baltic Sea and the Pacific Ocean. The dashed grey line represents the value of nitrous oxide at atmospheric equilibrium (Fig. 4b). Individual data points are plotted sequentially by increasing value. The same color symbol is used for each laboratory in all plots.



898  
899

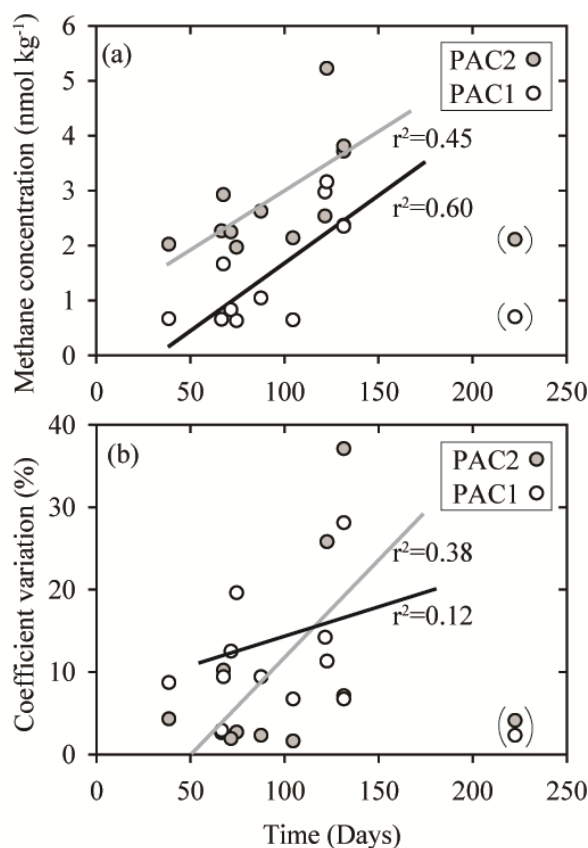
900 Figure 5. Deviation from the median value (reported in absolute units) for nitrous oxide datasets.  
 901 The batches of samples include BAL1,2,3,6,7 (Fig. 5a) and PAC2 and BAL5 (Fig. 5b). The  
 902 Baltic Sea samples are represented by circles and the Pacific Ocean samples are represented by  
 903 triangles. The shaded area indicates a deviation  $\leq 5\%$  from the median value, based on a water-  
 904 column concentration of  $11 \text{ nmol kg}^{-1}$  and  $42 \text{ nmol kg}^{-1}$  for Fig. 5a and 5b, respectively. The  
 905 color scheme for each laboratory dataset is identical to that used in Figure 4 and the letters  
 906 allocated to each dataset are to facilitate cross-referencing in the text. Note the y-axis for Fig 5a  
 907 and 5b are plotted on a different scale.



908

909 Figure 6. Three calibration curves for nitrous oxide measurements using an ECD including linear  
 910 (Fig. 6a), multilinear (Fig. 6b), and quadratic (Fig. 6c) fits.

911



912

913 Figure 7. Comparison of sample storage times with measured concentrations of methane (Fig.  
914 7a) and coefficient variation (Fig. 7b) for two sets of seawater samples (PAC1 and PAC2)  
915 collected in February 2017. These two sets of seawater samples had the lowest methane  
916 concentrations and appear to be influenced by the duration of storage time. The data points  
917 enclosed in parentheses were not included in the regression analysis. The PAC1 regression line  
918 is black and the PAC2 regression line is grey. All of the storage times are included in the  
919 Supplementary Material.